Towards Optical detection of magnon Nernst in $MnPS_3$

Chris Moore[1,2], John S. Jamison[2], Roberto C. Myers[2,3]
[1]*Department of Physics and Astronomy, The University of Washington, Seattle, WA, 98195, USA*
[2]*Department of Materials Science and Engineering, The Ohio State University, Columbus, OH, 43210, USA*
[3]*Department of Electrical and Computer Engineering, The Ohio State University, Columbus, OH, 43210, USA*

ABSTRACT

Magnon spin Nernst has been spatially resolved through doubly modulated detection of the magneto-optical Kerr effect (MOKE) in the material MnPS3. A temperature gradient is created in the collinear antiferromagnet $MnPS_3$ to induce magnon flows of opposite polarization in anti-parallel in-plane directions that are orthogonal to the gradient. This results in an induced spin current with a buildup of oppositely polarized magnon edge states. These edge states give rise to local surface magnetization which we probe for kerr rotation. This is the first documented optical detection of magnon spin nernst. Due to structural instabilities in the sample geometry a new sample stage was required to obtain higher confidence results. A new stage was designed and simulated in order to find the optimal material and geometry for a stable sample stage capable of inducing an appropriate temperature gradient through MnPS3. 200-250 words

I. Background and Introduction

Spin caloritronics is a subject within the greater field of spintronics, which chiefly studies the interactions between heat and the spin degree of freedom. Pure spin current has been studied in great detail through spin Hall, Seebeck, and Peltier effects but the spin Nernst effect was only recently observed. It was first seen in literature in late 2016[1][2] with proposed ideal materials for observation of $MnPS_3$ and its variants. Magnon Nernst was first detected using $MnPS_3$ one year later[3][4] through polarization sensitive thermopower voltage change in coupled Pt. We aim to show the first optical detection and spatial resolution of magnon Nernst using the magneto-optical kerr effect (MOKE).

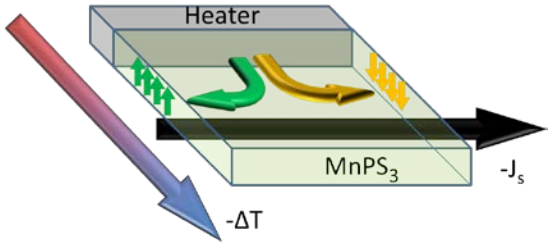

The magnon spin Nernst effect in $MnPS_3$. The path of the spin up (green) and spin down (orange) magnons is shown is in plane and orthogonal to the temperature gradient. This results in a net spin current in the direction of the spin up magnons.

$MnPS_3$ is a relatively unstudied material and little is known about its material coefficients, which are important to this experiment.

In order to control the heat flow within the basal plane of $MnPS_3$ a suspended heater geometry was used. The heater was fabricated by first depositing Silicon Nitride onto a silicon substrate, then

depositing Palladium by e-beam deposition and using e-beam lithography to etch this into a serpentine heater geometry. A wet etch with e-beam lithography is then used to create a trench beneath the heater. The samples were fabricated at UT Austin. Single crystals of $MnPS_3$ were grown by chemical vapor transport and are placed onto the heater by micromanipulators.

II. Methods

Experiments were conducted on a roughly 1000 μm^2 chemical vapor transport grown $MnPS_3$ sample that was placed by micromanipulators onto a suspended heater fabricated through a multi-step process involving electron beam lithography and focused ion beam milling. The sample was placed in an optical cryostat and probed utilizing the magneto-optical Kerr effect (MOKE) at temperatures from 5-78 K. To measure the MOKE we used a tunable Ti:Sapphire laser passed through a second harmonic generator to convert it to frequency-doubled photons. This beam is linearly polarized and incident normal to the sample where is the reflected beam passes through a Berek compensator (variable waveplate) and a Wollaston prism to split the horizontal and vertical polarizations onto a balanced photodiode bridge. The polarization rotation, measured as an intensity change in the balanced photodiode bridge, is proportional to the local magnetization in $MnPS_3$ due to spin accumulation at the edges. Wavelength is scanned to find the resonant transition in $MnPS_3$.

The signal at each of the photodiodes can be given as:

$$H = H_0 e^{i(\omega_c t+\phi_c)}(Th\, e^{i(\omega_h t+\phi_{th})} + k\, e^{i(\omega_h t+\phi_k)})$$

$$V = V_0 e^{i(\omega_c t+\phi_c)}(Th\, e^{i(\omega_h t+\phi_{th})} - k\, e^{i(\omega_h t+\phi_k)})$$

With H and V the horizontal and vertical polarization components respectively, detected separately at the photodiodes. The subscripts c, h, th, and k are for the laser chopper, heater, thermal reflectance, and Kerr respectively. The amplitudes Th and K are for thermal reflectance and Kerr respectively.

Using the lock in amplifier, we are able to distinguish the sum and difference of these signals at the chopper and heater frequencies:

$$(H+V)_c = A((H+V)_0 e^{i(\omega_c t+\phi_c)})$$

$$(H-V)_c = B((H-V)_0 e^{i(\omega_c t+\phi_c)})$$

$$(H+V)_h = A((H+V)_0 Th\, e^{i(\omega_h t+\phi_{th})} + (H-V)_0 k\, e^{i(\omega_h t+\phi_k)})$$

$$(H-V)_h = B((H+V)_0 k\, e^{i(\omega_h t+\phi_k)} + (H-V)_0 Th\, e^{i(\omega_h t+\phi_{th})})$$

With A=0.5 for our passive averager and B=26, the value of amplification on the difference channels.

To derive the kerr signal we first set about eliminating the thermal reflectance component:

$$\frac{(H+V)_h}{(H+V)_c} = Th\, e^{i((\omega_h-\omega_c)t+\phi_{th}-\phi_c)} + \frac{(H-V)_0}{(H+V)_0} k\, e^{i((\omega_h-\omega_c)t+\phi_k-\phi_c)}$$

$$\frac{(H-V)_h}{(H-V)_c} = Th\, e^{i((\omega_h-\omega_c)t+\phi_{th}-\phi_c)} + \frac{(H+V)_0}{(H-V)_0} k\, e^{i((\omega_h-\omega_c)t+\phi_k-\phi_c)}$$

$$\frac{(H+V)_h}{(H+V)_c} - \frac{(H-V)_h}{(H-V)_c} = k\, e^{i((\omega_h-\omega_c)t+\phi_k-\phi_c)}\left(\frac{(H-V)_0}{(H+V)_0} - \frac{(H+V)_0}{(H-V)_0}\right) =$$

$$k\, e^{i((\omega_h-\omega_c)t+\phi_k-\phi_c)}\left(\frac{B(H-V)_C}{A(H+V)_C} - \frac{A(H+V)_C}{B(H-V)_C}\right)$$

Isolating the complex kerr term gives:

$$ke^{i(\omega_k t+\phi_k)} = \frac{\frac{(H+V)_h}{(H+V)_c} - \frac{(H-V)_h}{(H-V)_c}}{\frac{B(H-V)_C}{A(H+V)_C} - \frac{A(H+V)_C}{B(H-V)_C}} e^{i(\omega_c t+\phi_c)} = \frac{AB((H+V)_h(H-V)_c - (H-V)_h(H+V)_c)}{(B(H-V)_c)^2 - (A(H+V)_c)^2} e^{i(\omega_c t+\phi_c)}$$

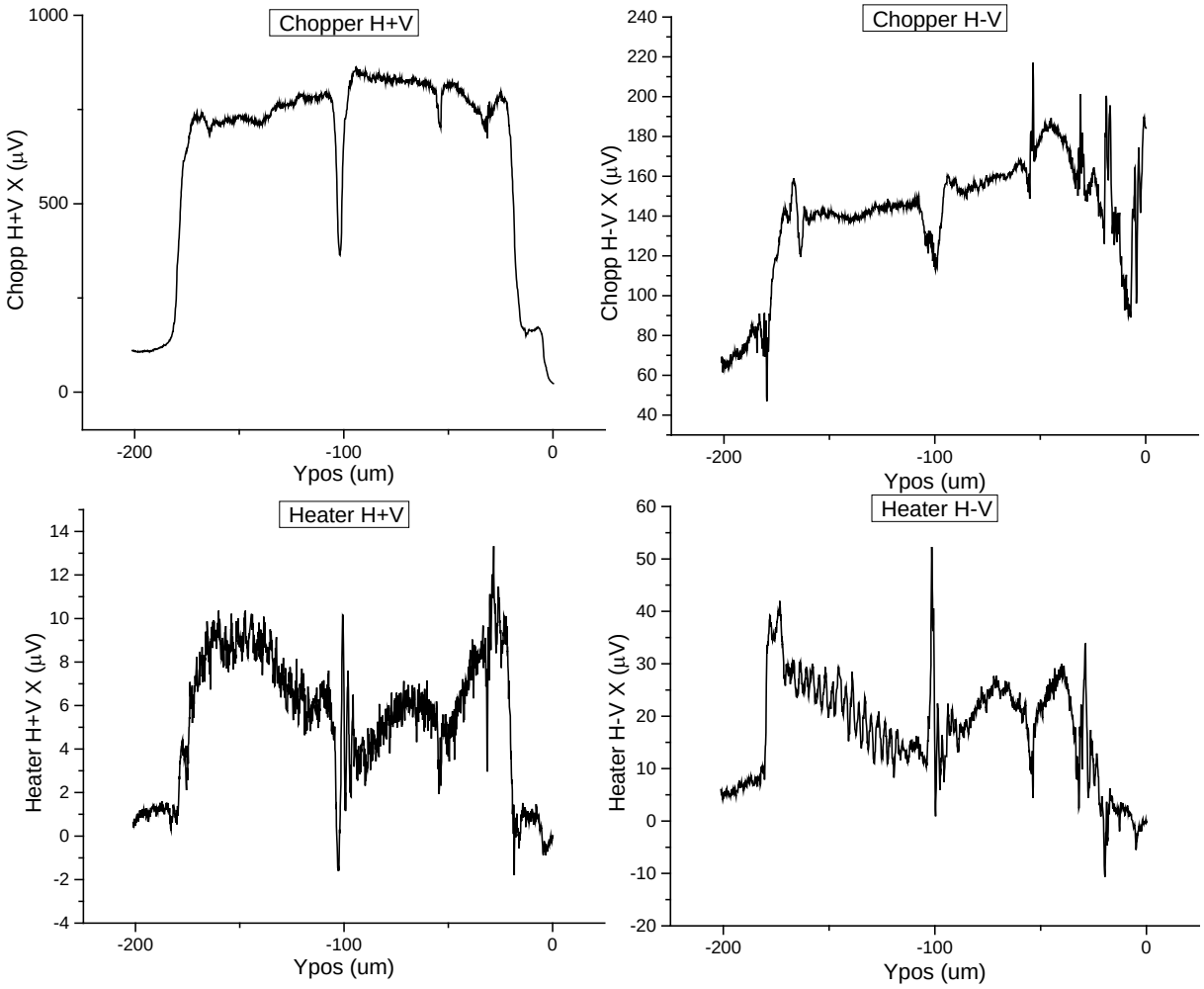

Plots of MOKE data from the first sample at a wavelength of 400nm incident on the sample surface showing all measurables without gains divided out.

Theoretically, we would expect the chopper difference term to be close to zero but due to a combination of scatter and vibrations in the sample mount, we were forced to take it into the general solutions.

In order to optimize our wavelength we swept through an incident-at-sample

wavelength range of 400 to 438 nm. We used the adjustability of our Ti-sapphire laser to take separate MOKE edge measurements at wavelength increments of 1 nm while reoptimizing the optical path for each wavelength and normalizing by intensity for each measurement. Upon comparison we were unable to ascertain a substantially larger peak kerr signal at any wavelength.

While troubleshooting we saw on the camera that the AC current through the heater was causing the heater to vibrate at the same frequency as the modulation of the current. This meant that our entire sample would also be vibrating at the frequency that we were trying to demodulate and therefor was corrupting our data.

III. Results and simulations

We used the linear fit of the optimization of the Berek compensator to convert units of voltage into kerr rotation. Upon examination of the data we still appear to have negative and positive peaks at the boundaries of the sample as we would expect. We are not, however, able to deduce easily the amount of contribution the vibration has to the data.

We have designed a new sample stage in order to continue the experiment while reducing any vibrational component. Comsol was used to design the new sample geometry and simulate multiple thermal conductivities for the insulator, heater, $MnPS_3$ in-plane, and $MnPS_3$ out-of-plane at 20K and 77K.

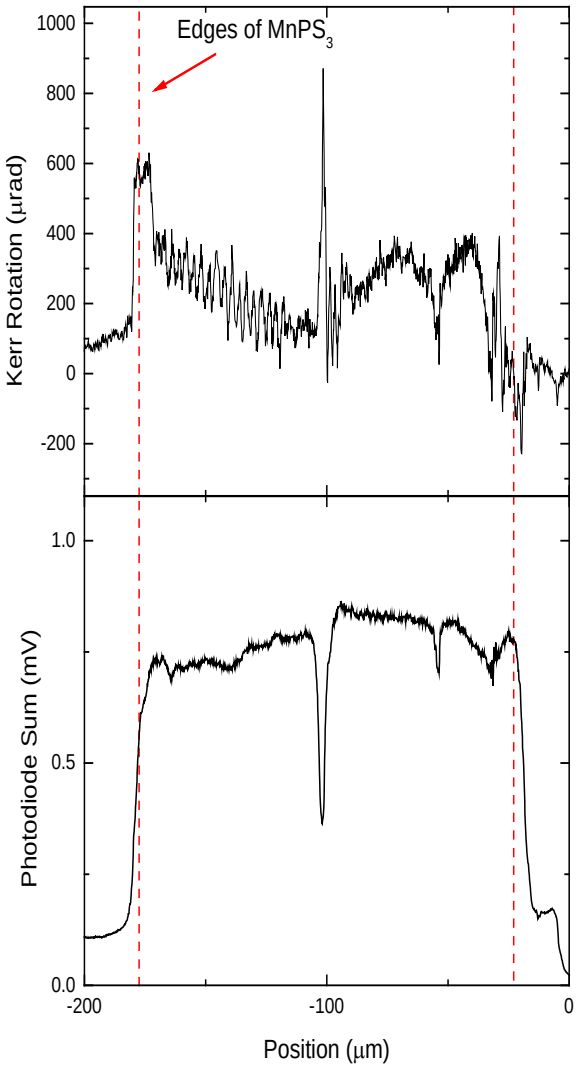

Kerr rotation of $MnPS_3$ sample from demodulated photodiode voltages and linear fit of Berek compensator.

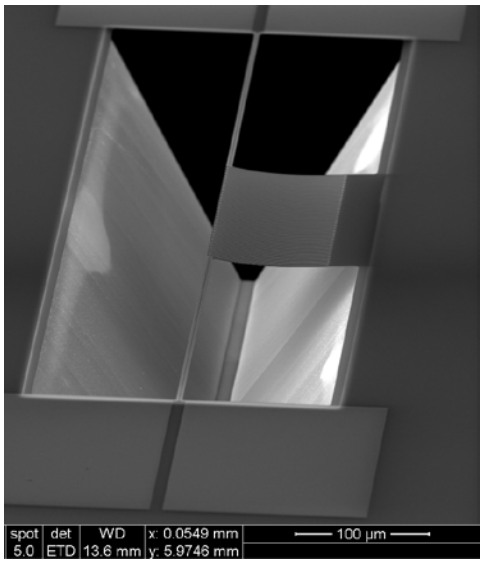

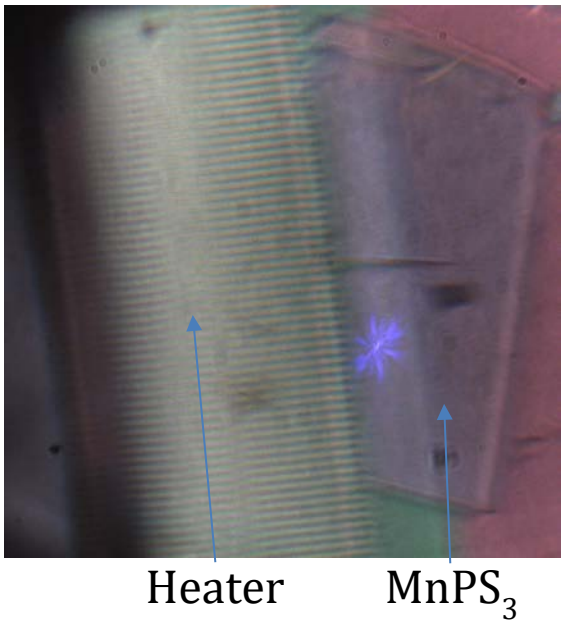

(left) SEM image of initial heater geometry showing fab of trough and suspended heater. (right) optical image showing the placement of $MnPS_3$ sample.

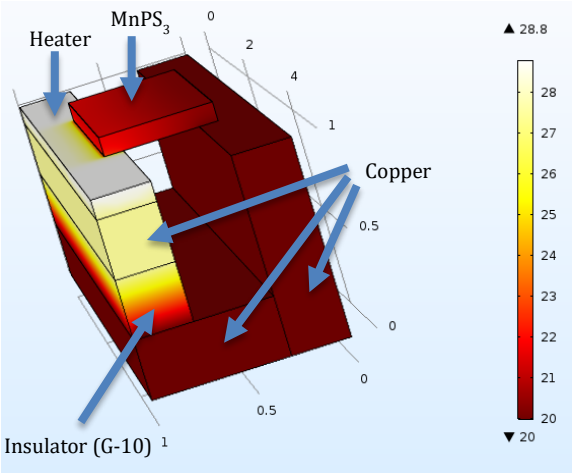

Comsol design of new sample mount

IV. Conclusions

We were able to detect photon polarization change in $MnPS_3$. Due to sample vibrations we were unable to determine what ratio of total polarization shift was due to the local magnetic edge states induced by the magnon nernst effect. These edge states of magnons are of particular interest to our group and therefore we set about redesigning the sample stage. A new stage was designed in Comsol and was simulated to find ideal components with a current ideal insulator of G-10. Further simulations must be done to match thermal expansion coefficients so that the sample stays flat while modulating the heater. Once simulations have been completed a new sample must be made and the experiment can be done again. We will also have the capacity with our current lock-in modulator to achieve time resolution of magnon diffusion by incorporating a delay line in our optical path.

V. Acknowledgments

I would like to thank John Jamison and Roberto Myers for their invaluable instruction and mentorship in this project.

I would also like to extend my appreciation to the NSF for providing the funding necessary for my participation in this Materials Research Science and Engineering Center (MRSEC) supported REU under NSF Award Number DMR-1420451.

VI. Footnotes, Endnotes and References

[1] V. A. Zyuzin and A. A. Kovalev. *Phys. Rev. Lett.* **117**, 217203 (2016)
[2] Cheng, Ran, S. Okamoto, and Di Xiao. *Physical Review Letters* **117**, 217202 (2016)
[3] S. Meyer, Y.-T. Chen, S. Wimmer, M. Althammer, T. Wimmer, R. Schlitz, S. Geprägs, et al. *Nature Materials* **16**, 977-81 (2017)
[4] Shiomi, Y., R. Takashima, and E. Saitoh. *Physical Review B* **96**, 134425 (2017)
[5] Grasso, V., F. Neri, P. Perillo, L. Silipigni, and M. Piacentini. *Physical Review B* **44**, 11060-66 (1991)